Available online at www.sciencedirect.com
ScienceDirect
Journal of Electrostatics 65 (2007) 542–548
Journal of ELECTROSTATICS
www.elsevier.com/locate/elstat

Observation and measurement of anomalous responses in a differential mobility analyzer caused by ultrafine fibrous carbon aerosols

Bon Ki Ku*, Andrew D. Maynard[1], Paul A. Baron, Gregory J. Deye

Centers for Disease Control and Prevention (CDC), National Institute for Occupational Safety and Health (NIOSH), 4676 Columbia Parkway, MS-R3, Cincinnati, OH 45226, USA

Received 25 August 2006; accepted 12 October 2006
Available online 12 March 2007

Abstract

We observed anomalous instrument responses above certain voltages when characterizing aggregates of airborne carbon nanotubes or nanofibers using a differential mobility analyzer (DMA). These were associated with sudden increases in measured number concentrations at high voltages, fluctuations in DMA voltage and audible high-frequency sounds from the DMA column. Onset of the anomalies depended on the material forming the aerosol and DMA sampling flow rate. The low density of the nanotubes relative to the nanofibers is thought to be the main reason the anomalous responses occur more easily and strongly with the nanotubes. Two possible mechanisms are suggested to explain the observations. The results indicate that measurement of nanometer-diameter conducting fibrous material by electrical mobility analysis may present a unique challenge.

Keywords: Carbon nanotube/nanofiber; Differential mobility analyzer; Electrical discharge; Arcing; Low density

1. Introduction

The mobility-based size measurement method is widely used by itself or combined with other instruments in applications such as nano-sized atmospheric particulate matter monitoring [1], diesel exhaust analysis [2], characterization and evaluation of nanoparticle size standards below 10 nm [3,4], and studies of nanostructured material exposure during handling and manufacturing [5]. A differential mobility analyzer (DMA), based on electrical mobility separation of particles [6], extracts particles with a narrow range of mobilities out of an input flow including particles of many sizes and charges. The DMA combines the axial laminar flow field and the radial electric field formed between two concentric cylinders to separate charged nanoparticles in space rather than in time.

In recent years, carbon-based nanotubes/nanofibers have become a focal point of research. Several different processes and types of tubes/fibers have been developed, with special interest as the tube/fiber diameters approach the nanometer range. Single-walled carbon nanotubes (SWCNTs) consist of a single layer of carbon atoms in a cylindrical arrangement, resulting in structures about 1.4 nm in diameter and up to a millimeter or more in length [7,8]. Carbon nanofibers (Pyrograf® III) [9] are formed as stacked conical layers of graphitic carbon and they have diameters nominally in the range of 60–150 nm and can be many micrometers long. These nanofibers are much smaller in diameter than conventional continuous or milled carbon fibers (5–10 μm) but significantly larger than carbon nanotubes (CNTs) (1–10 nm) [9].

From a health perspective, there is growing concern over the potential adverse health effects of these particles [5,10,11]. Past industrial experience with asbestos has called attention to the potential hazards associated with small diameter fibers [12]. A recent review of engineered nanomaterial toxicity tests emphasized the need to fully characterize airborne CNTs in the submicrometer size

*Corresponding author. Tel.: +1 513 841 4147; fax: +1 513 841 4545.
E-mail address: BKu@cdc.gov (B.K. Ku).
[1]Current address: Woodrow Wilson International Center for Scholars, Project on Emerging Nanotechnologies, One Woodrow Wilson Plaza, 1300 Pennsylvania Avenue NW, Washington, DC 20004, USA.

0304-3886/$ - see front matter © 2007 Elsevier B.V. All rights reserved.
doi:10.1016/j.elstat.2006.10.012

range, e.g., size distribution measurement using a DMA (see Table 3 in [13]).

Measurement of nanometer-diameter conducting fibrous particles by electrical mobility analysis may present a unique challenge because such particles have very low effective density. Baron and co-workers briefly mentioned their experience with electrical discharge in a fiber classifier that used dielectrophoresis to separate fibers by length [14,15]. This classifier was internally coated with an oil/grease mixture to prevent fiber deposition-related disturbances in the flow or electrical fields. Large carbon fibers (geometric mean diameter 3.74 μm, geometric mean length 35 μm) were classified in a mobility analyzer [16] very similar to the one used in the present study. The fibers were deposited on plastic strips covering the inner electrode, but no anomalous discharging or arcing effects were noted [16].

In this study, anomalous DMA behavior was clearly observed when characterizing airborne carbon nanotubes or nanofibers using a DMA. Observed behaviors, which were associated with sudden increases in measured number concentrations at high voltages, fluctuations in DMA voltage and audible high-frequency sounds from the DMA column, have not been reported for other nanoparticles. Therefore, in this study, we investigated how the airborne CNT aerosols generated through agitation from a laboratory vortex shaker produced the anomalous DMA response for different aerosol flow rates and material types.

2. Experimental

2.1. Aerosol generation

The experimental setup for this study is shown in Fig. 1. As-produced high-pressure carbon monoxide (HiPCO®) materials (Carbon Nanotechnologies Inc. (CNI)) or Pyrograf® III material (Type PR-24, Grade LHT, Applied Sciences Inc.) were aerosolized using the method previously described [5]. In this paper, the HiPCO® materials from two batches were referred to as HiPCO® A and HiPCO® B. HiPCO® A was produced some months before HiPCO® B and the process was modified slightly in between batches. Fibrous carbon nanoparticles aerosolized by a vortex shaker were introduced to a Po-210 neutralizer to provide a Boltzmann equilibrium charge distribution before entering the DMA. The mobility-based size distributions of polydisperse fibrous carbon aerosols were measured using a scanning mobility particle sizer (SMPS; TSI Inc.) with an impactor (50% cut diameter of 0.0457 cm diameter impactor is about 0.7 μm at 0.3 l/min of aerosol flow rate) and a condensation particle counter (CPC; Model 3022a, TSI Inc.). Monodisperse particles were generated using a DMA (3081, TSI Inc.) which is a component of the SMPS to select the ultrafine carbon particles of a predetermined mobility diameter for sampling and TEM measurement. Particle sampling was performed using an impactor-based electrostatic precipitator [17]. After running the DMA with each material, the DMA was thoroughly cleaned to exclude contamination of the DMA by the material previously used.

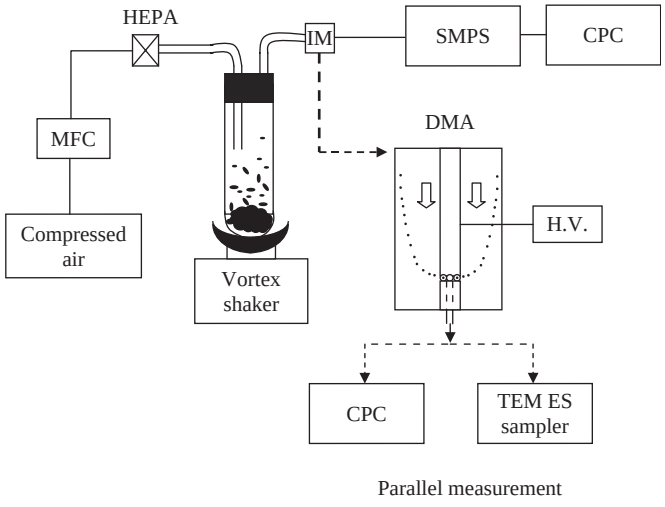

Fig. 1. Experimental setup. MFC: mass flow controller; HEPA: high efficiency particulate air filter; SMPS: scanning mobility particle sizer; DMA: differential mobility analyzer; CPC: condensation particle counter; TEM: transmission electron microscope; ES: electrostatic; IM: impactor; H.V.: high voltage power supply.

2.2. Carbon-based ultrafine fibrous materials

Images of HiPCO® and Pyrograf® III particles are presented in Fig. 2. The HiPCO® and Pyrograf® materials are different in several respects. The structure of the HiPCO® SWCNT particles (Figs. 2a and b) was observed to be bundles of individual nanotubes (single molecules) self-assembled into ropes (approximately from about 2 nm to greater than 50 nm in diameter) which can splay apart and form much larger expanded structures. The Pyrograf® III nanofibers on the other hand were found to be much larger in diameter (50–200 nm) [18] and are formed as stacked conical layers of graphitic carbon. Individual fibers are clearly visible and do not self-organize into well-defined bundles, but rather tend to attach more randomly to each other as matted material as shown in Figs. 2c and d.

2.3. Measurement protocols

DMA anomalous response was investigated under several experimental conditions. Anomalous behavior onset was defined as a voltage at which sudden increases in measured number concentration were recorded. Other indications of anomalous response included an audible clicking that suggested arcing, and fluctuations in the high voltage analyzer output. Aerosol flow rate was varied from 0.3 to 1.0 l/min to evaluate the effect of the flow rate on onset of anomalous behavior. Material-type dependence of the anomaly was also examined at a fixed flow rate.

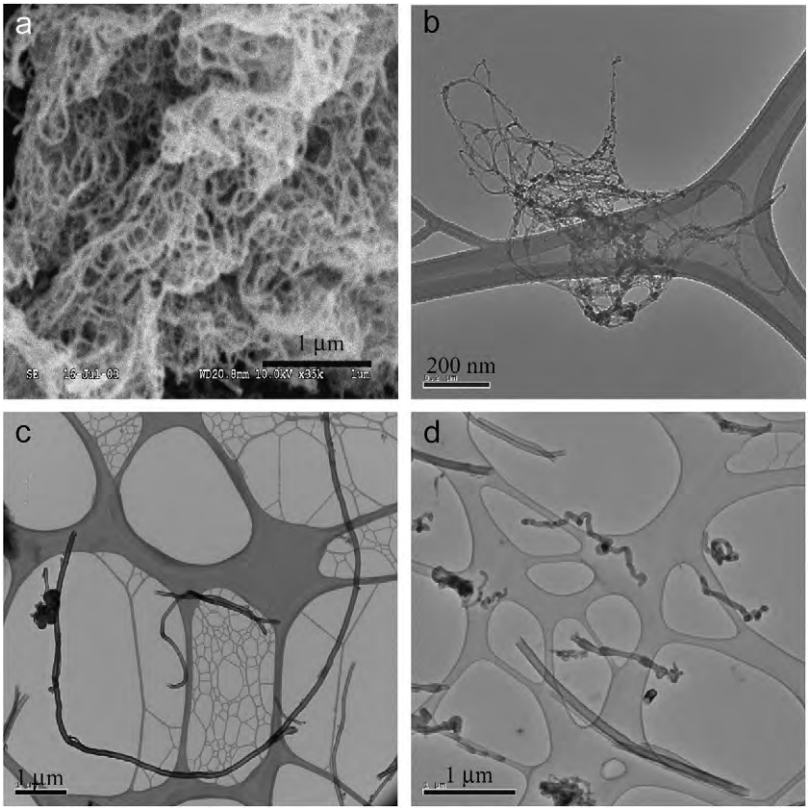

Fig. 2. SEM/TEM micrographs of typical particles: (a) polydisperse clumps of bulk material sample (SEM image) and (b) aerosolized 150 nm mobility size particles (TEM) for HiPCO® materials, (c) aerosolized polydisperse particles (TEM), and (d) aerosolized 200 nm mobility size particles (TEM) for Pyrograf® III material.

3. Results and discussion

3.1. Observation of anomalous DMA response

The carbon-based ultrafine fiber aerosols generated through agitation caused anomalous increases in recorded concentration for all materials we tested. We had not experienced this kind of DMA behavior for other nanoparticles such as metals or metal oxides. This anomalous DMA response is apparently caused by the unique attributes of ultrafine fibrous carbon material.

An anomalous and significant increase (about one to two orders of magnitude) in measured concentration of ultrafine carbon fibrous particles was observed for several different conditions (Fig. 3). The difference between an unusual increase in the number concentration and the real number concentration variation could be distinguished by the fact that the number concentration caused by anomalous response was one or two orders of magnitude higher than that of the real concentration. Fig. 3a clearly shows suddenly increased number concentrations for HiPCO® A, which is due to CNT arcing at about 6000 V in the DMA for an aerosol flow rate of 0.3 l/min. Fig. 3b also shows a similar phenomenon occurring at a much lower DMA voltage, 1000 V, for HiPCO® B at 1.0 l/min. As shown in Figs. 3a and b, the number concentration of the CNT aerosols generated by the vortex shaker is relatively low, i.e., on the order of 10 particles/cm^3 per channel and the one due to the arcing is at the level of several hundred particles/cm^3. The low aerosol generation rate from the HiPCO® material powder may be due to the properties of low bulk density and fluffiness of the material. Fig. 3c shows the number concentration measured for Pyrograf® III at 1.0 l/min. DMA voltages related to the sudden increase in the concentrations are 8000 and 900 V, indicating that anomalous response can occur at very different DMA voltages, which is possibly related to the degree of deposition of the fibrous particles in the DMA during the DMA runs. On the other hand, at lower flow rate of 0.3 l/min Pyrograf® III showed little evidence on the anomalous response. At the University of Minnesota, a laboratory test was performed under similar conditions without the impactor at the inlet of the DMA. In these runs, there was arcing observed at a very low DMA voltage. For the case without an impactor, it was only possible to obtain a size distribution up to several hundred volts because of severe arcing (data not included here). The arcing voltage was about 200 V. Based on these experiments, the anomalous response of the DMA without the impactor is believed to be triggered by larger clumps introduced into the DMA. The anomalous response intensity of the DMA appears to depend on physical

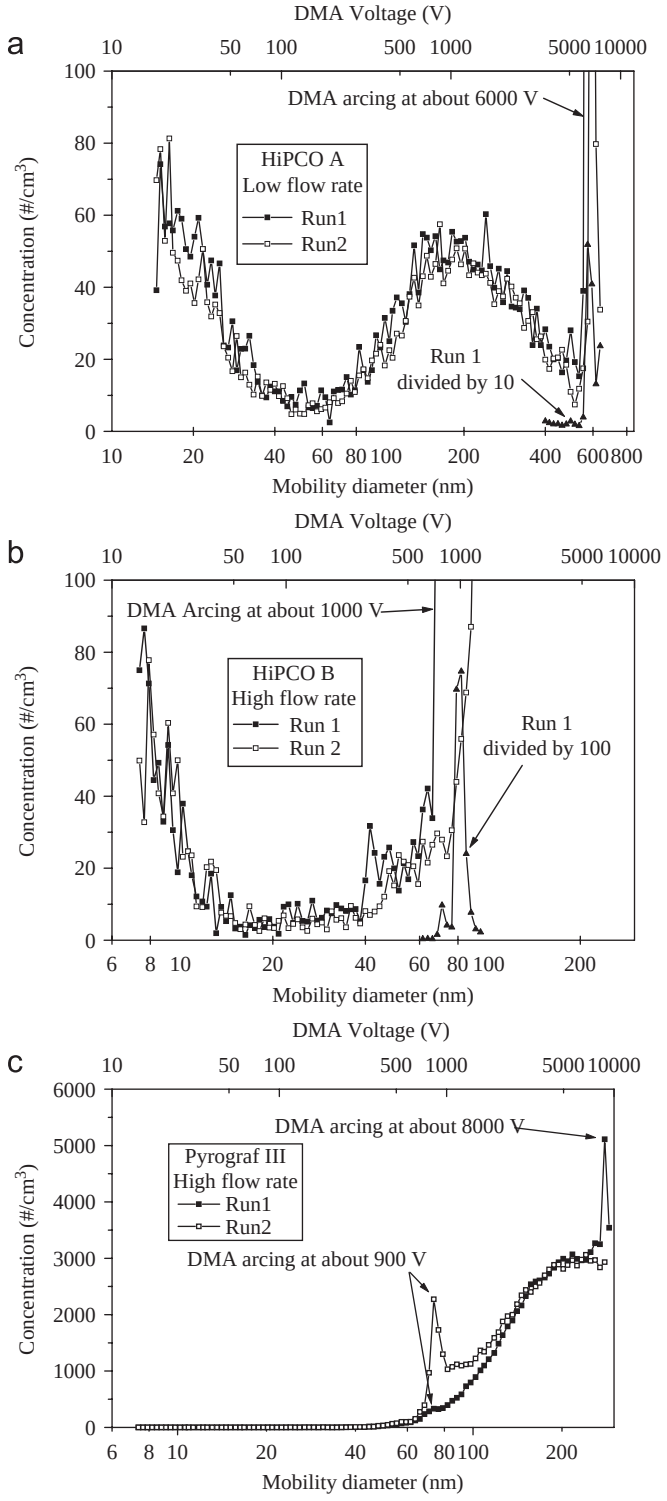

Fig. 3. Number concentrations measured (a) for HiPCO® A material, (b) for HiPCO® B material, and (c) for Pyrograf® III material, showing clearly abnormally sudden increase in the concentration due to arcing in the DMA. Aerosol flow rate was 0.3 and 1.0 l/min for HiPCO® A and HiPCO® B/Pyrograf® III, respectively. Another graph of the original data divided by some scale factor was added to the main figure to show relative magnitude of anomalous responses. Note that HiPCO® material shows stronger anomalous response than Pyrograf® III and anomaly onset voltage in (b) is lower than for the lower aerosol flow rate shown in (a).

properties of each material and it was caused relatively easily by the HiPCO® materials compared to the Pyrograf® III material. The reason for the different response between them seems to be the lower effective density of the HiPCO® materials, which may allow larger clumps to go through the impactor to the DMA while larger particles of the Pyrograf® III were removed by the impactor. TEM observation of HiPCO® materials as shown in Figs. 2a and b confirmed this fact and recent studies identified much lower density of HiPCO® materials than Pyrograf® III material [18,19], resulting in HiPCO® material particles having much larger physical diameters than mobility diameters. Therefore, the fact that the low concentration of the order of 1000 particles/cm^3 in total for HiPCO® materials can cause an anomalous response in the DMA after running the DMA only several times, presents a unique challenge. For example, the concentration of about 1000 particles/cm^3 in total flowing through the DMA at 1 l/min for about the 6 min (2 min time was used for each run of the DMA in this study) needed to observe anomalous responses indicates that only several million particles can produce this effect. This makes the problem unique for ultrafine fibrous carbon aerosols since no other nanoparticles such as welding particles and combustion particles were reported to cause the same problem with such a low level of aerosols. It is interesting that no anomalous problems were noted in the DMA in a gas metal arc welding study even though the welding particles are chainlike and conductive, and the number concentrations are pretty high, i.e., over 1,000,000 particles/cm^3, compared to the fibrous particles in this study [20].

As briefly mentioned above, the observance of these anomalous measurements was reduced significantly for an aerosol in which most of the larger particles were removed by settling and impaction. Baron et al. [21] observed that HiPCO® CNT powder exhibited extremely low bulk density (about 0.01 g/cm^3). Recently, Ku et al. [18] showed that monodisperse Pyrograf® III particles in the size ranging from 100 to 700 nm have densities decreasing from 1.2 to 0.4 g/cm^3. Maynard et al. [5] observed that because of this low density, HiPCO® nanotubes were not effectively deposited on impactor stages; the particles were simply swept off the surface of the impaction substrate. DMAs normally depend on an impactor at the inlet to remove particles larger than a selected size (for instance, 50% cut diameter of 0.0457 cm nozzle diameter impactor is about 0.7 μm for the SMPS and 0.5 μm for the wide-range particle spectrometer (WPS; MSP Inc., St. Paul, MN) at 0.3 l/min of aerosol flow rate). Thus, it is likely that large particle penetration into the classifier region may cause disruption in the electric and flow field inside the classifier.

3.2. Effect of aerosol flow rate on anomalous DMA response

Table 1 summarizes the statistics for onset voltages of DMA anomaly for HiPCO® A&B and Pyrograf® III at two different flow rates. Higher aerosol flow rate causes

Table 1
Summary of statistics for onset voltages of DMA anomaly

Run	Material	Flow rate (l/min)	Onset voltage (V)	Concentration (particles/cm^3)	Mean (V)	Standard deviation
1	HiPCO® A	0.3	6000	3.18e3	5960	920
2	HiPCO® A	0.3	6300	2.86e3		
3	HiPCO® A	0.3	4400	3.97e3		
4	HiPCO® A	0.3	6300	3.03e3		
5	HiPCO® A	0.3	6800	1.57e3		
1	HiPCO® A	1.0	3200	698	3900	990
2	HiPCO® A	1.0	4600	131		
1	HiPCO® B	0.3	5500	329	5120	1010
2	HiPCO® B	0.3	5200	335		
3	HiPCO® B	0.3	6500	391		
4	HiPCO® B	0.3	4600	450		
5	HiPCO® B	0.3	3800	213		
1	HiPCO® B	1.0	840	1.16e3	1110	460
2	HiPCO® B	1.0	1390	1.38e3		
3	HiPCO® B	1.0	430	650		
4	HiPCO® B	1.0	1480	1.86e3		
5	HiPCO® B	1.0	1390	1.02e3		
1	Pyrograf® III	1.0	890	8.37e4	890[a]	55
2	Pyrograf® III	1.0	840	8.19e4		
3	Pyrograf® III	1.0	950	7.11e4		
4	Pyrograf® III	1.0	8100	7.11e4		

[a]This mean voltage was calculated with the first three data.

DMA arcing at lower voltages, 3900 and 1100 V, respectively, for HiPCO® A&B materials, while for Pyrograf® III anomalous response was observed in a way that it occurred at both lower and high voltages, 900 and 8000 V as shown in Fig. 3c. It is noteworthy that the aerosol flow rate affects arcing onset voltage, actually, lowering it, suggesting that a low flow rate should be used to delay the arcing toward higher DMA voltages. Even though the aerosol generation rate is relatively low at the order of 10 particles/cm^3 per size bin, as shown in Figs. 3a and b, compared to other aerosols such as hydrocarbon and metal oxides generated by combustion and furnace processes, it is high enough to cause arcing in the DMA [22]. As for the reason of the lower arcing onset voltage at a higher flow rate with HiPCO® materials, it is hypothesized that higher aerosol flow provides a greater amount of CNT aerosols into the DMA relative to the lower flow and so more CNT particles could deposit and accumulate on the DMA electrode surface, which would possibly act as a point source for arcing.

3.3. Electrostatically based mechanisms in the DMA

We have made several observations on anomalous measurements of carbon-based ultrafine fibrous particle aerosols, suggesting that electrical effects are the basis of these effects. Baron et al. briefly mentioned their experience with a similar situation in the fiber classifier [14], but they did not report any possible mechanism in the paper. We are also still not clear on all the potential mechanisms because we cannot directly see what happens inside the classifier. However, we will attempt to suggest mechanisms that are consistent with our observations as well as that of others in electrostatically based systems. The audible noise certainly suggests arcing inside the classifier. The increase in current in the high voltage supply to the DMA suggests either arcing or corona discharge within the classifier. The increase in apparent concentration at a certain voltage suggests two possibilities. First, the electrical noise from arcing or corona discharge could affect the detection system and produce an increase in count rate. Alternatively, there are several mechanisms that could mix the aerosol inside the classifier so that a whole range of particle sizes could reach the exit slit normally reserved only for the classified particles. This would increase the apparent concentration quite significantly. There may be also the possibility of particle generation during arcing—either from the nanotubes/fibers, or the DMA wall.

The presence of electrical arcing within the classifier can cause mixing of the aerosol and sheath flows and can allow normally non-selected particles to exit through the classified particle slit. In addition, this arcing is potentially damaging to the electronics of the classifier. If a corona discharge occurs from deposited particles, the corona wind can also mix the aerosol/sheath flows and result in anomalous increased particle detection.

Both the CNTs and the carbon nanofibers are made of highly conductive material. When highly asymmetric

(having an aspect ratio (length/diameter) much greater than 1.0) conductive particles are placed in an electric field, the particles will align with their long axis parallel to the field lines [12]. When these particles, or especially fibers, reach the electrode surface, they initially attach to the surface, aligned so that they stick normal to the surface. If both the particle and surface are conductive, the particle will become highly charged and experience a repulsive force from the surface. If the surface is coated with an oil (as in [15]), the surface is no longer conductive and the fibers stick to the surface. Alternatively, if it sticks to the surface, it may act as a point source for corona discharge or arcing (Fig. 4a). Otherwise, the fiber, with only a small area for adhesive forces to operate, is likely to detach from the surface and accelerate to the opposite electrode. This process can be repeated at the opposite electrode though slightly downstream, since the particle experiences the flow field while transiting from one electrode to the other. The particle thus bounces between electrodes and makes its way down the classifier. Similar motion has been described for commercial electrostatic flocking and sandpaper production facilities [23]. These particles may reach the classified particle exit slit. Alternatively, if a sufficient number of particles bounce between the electrodes, the particle motion may mix the aerosol/sheath flow, allowing normally non-classified particles to mix into the classified particle flow (Fig. 4b). Schematic diagram about these two possible mechanisms is shown in Fig. 4a and b. It is possible that both of these mechanisms described above may be occurring, since sometimes there occurs an increase in current associated with a number concentration, and other times not. For instance, if the disturbance in the size distribution observed is caused by arcing (presumably from a deposit in the classifier as shown in Fig. 4a), it should be present regardless of whether additional particles are introduced or not.

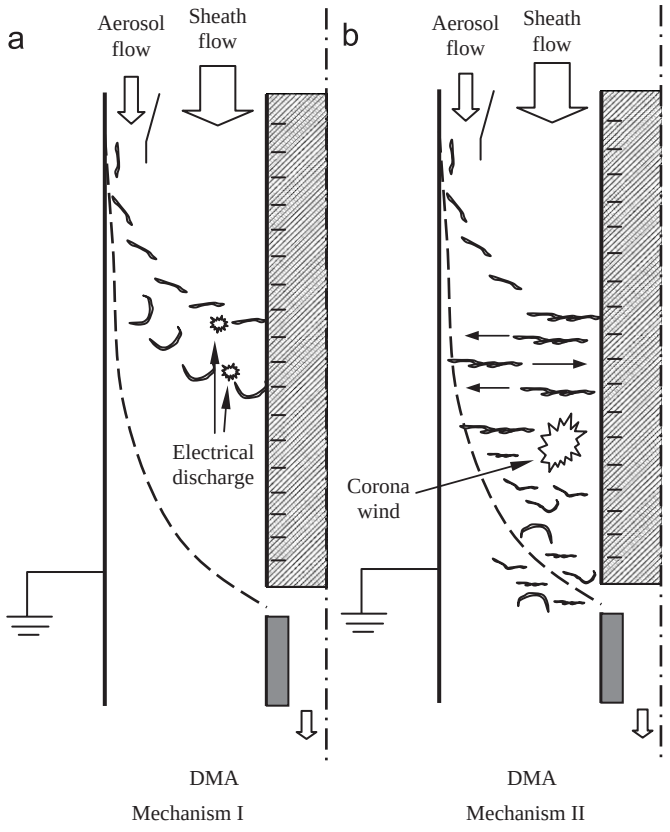

Fig. 4. Two possible mechanisms on anomalous responses in the DMA: (a) arcing caused by particles being deposited on the DMA electrode surface and (b) mixing of aerosol and sheath flows by either corona wind or particles moving back and forth as they travel downward in the DMA. Both the corona wind and the accelerating particles back and forth may cause mixing of aerosol/sheath air stream. When the aerosol stream is mixed, particles of all sizes could reach the exit slit for the classified particles and cause a large increase in particles detected. Particles introduced into the DMA were exaggerated in their sizes for a simple explanation about arcing. The corona wind is likely to be produced from fibers attached to the walls, just as the arcing is. The picture (b) does not indicate this.

The anomalous results observed in each of the instruments can be explained by invocation of several general observations. The lack of adequate classification of the incoming aerosol can result in large clumps of material entering the classifier and causing the anomalous results. Increasing the flow to the classifier decreases the observed voltage of the anomalous results (as shown in Fig. 3). This is a bit more difficult to understand, but may be caused by increased penetration of large clumps of material. The significantly lessened observation of anomalous results in the WPS was perhaps the result of elimination of most of the large clumps by an external settling chamber (not described in Section 2).

4. Conclusions

Anomalous responses above certain voltages were observed in a DMA when characterizing aggregates of airborne carbon nanotubes or nanofibers. Onset of the anomalies depended on the material forming the aerosol and sampling flow rate. The anomalous behavior is associated with a sudden increase in measured number concentration, fluctuations in the high voltage analyzer output and audible high-frequency sounds from the DMA column. The fluffiness and low density of the HiPCO® materials relative to Pyrograf® III is believed to be the main reason arcing occurs more easily and strongly with the HiPCO® product. Two possible mechanisms associated with the anomalous behavior include: one is arcing caused by particles being deposited on the DMA electrode surface and the other is mixing of aerosol and sheath flows either by corona wind produced from particles attached to the electrode or by particles moving back and forth as they travel downward in the DMA, which may disrupt the aerosol and sheath flows. The results indicate that measurement of nanometer-diameter conducting fibrous material by electrical mobility analysis may present a unique challenge.

Acknowledgments

We would like to thank Mr. Mark S. Emery and Dr. Mark R. Stolzenburg at University of Minnesota for assisting in running a DMA without an impactor for the Pyrograf® III material.

Disclaimer: The mention of any company or product does not constitute an endorsement by the Centers for Disease Control and Prevention. The findings and conclusions in this report are those of the authors and do not necessarily represent the views of the National Institute for Occupational Safety and Health.

References

[1] P.H. McMurry, X. Wang, K. Park, K. Ehara, The relationship between mass and mobility for atmospheric particles: a new technique for measuring particle density, Aerosol Sci. Technol. 36 (2) (2002) 227–238.
[2] C.V. Gulijk, J.C.M. Marijnissen, M. Makkee, J.A. Moulijn, A. Schmidt-Ott, Measuring diesel soot with a scanning mobility particle sizer and an electrical low-pressure impactor: performance assessment with a model for fractal-like agglomerates, J. Aerosol Sci. 35 (2004) 633–655.
[3] B.K. Ku, J. Fernandez de la Mora, Cluster ion formation in electrosprays of acetonitrile seeded with ionic liquids, J. Phys. Chem. B 108 (2004) 14915–14923.
[4] B.K. Ku, J. Fernandez de la Mora, D.A. Saucy, J.N. Alexander IV, Mass distribution measurement of water-insoluble polymers by charge-reduced electrospray mobility analysis, Anal. Chem. 76 (2004) 814–822.
[5] A.D. Maynard, P.A. Baron, M. Foley, A.A. Shvedova, E.R. Kisin, V. Castranova, Exposure to carbon nanotube material: aerosol release during the handling of unrefined single walled carbon nanotube material, J. Toxicol. Environ. Health 67 (1) (2004) 87–107.
[6] E.O. Knutson, K.T. Whitby, Aerosol classification by electric mobility: apparatus, theory, and applications, J. Aerosol Sci. 6 (6) (1975) 443–451.
[7] S. Subramoney, Novel nanocarbons—structure, properties, and potential applications, Adv. Mater. 10 (15) (1998) 1157.
[8] S.B. Sinnott, R. Andrews, Carbon nanotubes: synthesis, properties, and applications, Crit. Rev. Solid State Mater. Sci. 26 (3) (2001) 145–249.
[9] Applied Sciences Inc., 〈http://www.apsci.com/ppi-pyro3.html〉.
[10] A.A. Shvedova, E.R. Kisin, R. Mercer, A.R. Murray, V.J. Johnson, A.I. Potapovich, Y.Y. Tyurina, O. Gorelik, S. Arepalli, D. Schwegler-Berry, A.F. Hubbs, J. Antonini, D.E. Evans, B.K. Ku, D. Ramsey, A. Maynard, V.E. Kagan, V. Castranova, P. Baron, Unusual inflammatory and fibrogenic pulmonary responses to single walled carbon nanotubes in mice, Am. J. Physiol. Lung Cell. Mol. Physiol. 289 (2005) L698–L708.
[11] A.A. Shvedova, E.R. Kisin, A.R. Murray, V.Z. Gandelsman, A.D. Maynard, P.A. Baron, V. Castranova, Exposure to carbon nanotube material: assessment of the biological effects of nanotube materials using human keratinocyte cells, J. Toxicol. Environ. Health 66 (20) (2003) 1909–1926.
[12] P.A. Baron, C.M. Sorensen, J.E. Brockman, Nonspherical particle measurements: shape factors, fractals, and fibers, in: P.A. Baron, K. Willeke (Eds.), Aerosol Measurement: Principles, Techniques, and Applications, second ed., Wiley, New York, 2001, pp. 705–749.
[13] G. Oberdörster, A. Maynard, K. Donaldson, V. Castranova, J. Fitzpatrick, K. Ausman, J. Carter, B. Karn, W. Kreyling, D. Lai, S. Olin, N. Monteiro-Riviere, D. Warheit, H. Yang, Principles for characterizing the potential human health effects from exposure to nanomaterials: elements of a screening strategy, Part. Fiber Toxicol. 2 (2005).
[14] P.A. Baron, G.J. Deye, J. Fernback, Length separation of fibers, Aerosol Sci. Technol. 21 (1994) 179–192.
[15] G.J. Deye, P. Gao, P.A. Baron, J.E. Fernback, Performance evaluation of a fiber length classifier, Aerosol Sci. Technol. 30 (1999) 420–437.
[16] B.T. Chen, H.-C. Yu, C.H. Hobbs, Size classification of carbon fiber aerosols, Aerosol Sci. Technol. 19 (1993) 109–120.
[17] B.K. Ku, A.D. Maynard, Comparing aerosol surface-area measurement of monodisperse ultrafine silver agglomerates using mobility analysis, transmission electron microscopy and diffusion charging, J. Aerosol Sci. 36 (2005) 1108–1124.
[18] B.K. Ku, M.S. Emery, A.D. Maynard, M.R. Stolzenburg, P.H. McMurry, In situ structure characterization of airborne carbon nanofibers by a tandem mobility-mass analysis, Nanotechnology 17 (2006) 3613–3621.
[19] A.D. Maynard, B.K. Ku, M.S. Emery, M.R. Stolzenburg, P.H. McMurry, Measuring particle size-dependent physicochemical structure in airborne single walled carbon nanotube agglomerates, J. Nanoparticle Res. 9 (2007) 85–92.
[20] A.T. Zimmer, P. Biswas, Characterization of aerosols resulting from arc welding processes, J. Aerosol Sci. 32 (2001) 993–1008.
[21] P.A. Baron, A.D. Maynard, A. Shvedova, V. Castranova, E. Kisin, A. Murray, V. Gandelsman, M. Foley, Preliminary studies of generation, exposure, and toxicity of carbon nanotube, in: Abstracts of the 22nd Annual AAAR Conference, Anaheim, CA, October 20–24, 2003, p. 161.
[22] B.K. Ku, A.D. Maynard, P.A. Baron, G. Deye, Anomalous responses (arcing, electrical discharge) in a differential mobility analyzer caused by ultrafine fibrous carbon aerosols, in: Abstracts of the 24th Annual AAAR Conference, Austin, TX, October 17–21, 2005, p. 43.
[23] A.D. Moore, Electrostatics and its Applications, Wiley, New York, 1973.